

Solubility Behavior, Phase Transition, and Structure-Based Nucleation Inhibition of Etanidazole in Aqueous Solutions

Michael B. Maurin,^{1,2} Susan M. Rowe,¹ Kenneth S. Field,¹ Robert C. Swintosky,¹ and Munir A. Hussain¹

Received January 8, 1996; accepted June 11, 1996

Purpose. The solubility behavior, phase transition and inhibition of the nucleation process of etanidazole were characterized.

Methods. Solubility measurements as a function of time permitted characterization of the solubility behavior and phase transition. The precipitate from saturated solutions was isolated and characterized by differential scanning calorimetry, polarized light microscopy, x-ray powder diffraction and coulometric analysis. The physical stability of metastable systems was examined in the presence of various structure-based nucleation inhibitors.

Results. Etanidazole is soluble in water with an equilibrium solubility of 68.1 mg/mL, pH 6.5 with changes in pH having virtually no effect on the solubility. Etanidazole reaches concentrations in excess of 150 mg/mL within one hour. Etanidazole solutions prepared at 150 mg/mL contained crystals after rotating for 24 hours. The crystals were isolated and characterized as etanidazole monohydrate. The solubility of etanidazole monohydrate in water increased with time reaching an equilibrium solubility of 68 mg/mL after 24 hours. Therefore, the solubility studies were actually determining the solubility of the more stable monohydrate form of etanidazole. Etanidazole solutions at concentrations of 50, 100 and 150 mg/mL were stabilized to varying degrees with structure-based nucleation inhibitors (imidazole, ethanolamine or diethanolamine).

Conclusions. Anhydrous etanidazole undergoes a transition in aqueous solutions to the more stable monohydrate when the solubility of the monohydrate is exceeded. The physical stability of etanidazole solutions at 4°C is improved following autoclaving. The addition of structure-based nucleation inhibitors effectively stabilized the metastable systems.

KEY WORDS: etanidazole; solubility behavior; phase transition; hydrate formation; nucleation inhibition.

INTRODUCTION

Etanidazole (*N*-(2-Hydroxyethyl)-2-nitro-1*H*-imidazole-1-acetamide, SR-2508, DuP 435) is a member of the nitroimidazole class of radiosensitizers/chemosensitizers that are under evaluation as adjuvant therapy in solid tumor treatment (Fig. 1) (1,2). The nitroimidazoles sensitize hypoxic tumor cells to radiation and alkylating cytotoxic agents (3,4). The mechanism of action appears to rely on the depletion of intracellular glutathione (5) and inhibition of glutathione transferases (6), thereby, enhancing sensitivity to radiation and alkylating agents.

The seminal work of Shefter and Higuchi characterized the dissolution behavior and thermodynamics of several organic pharmaceuticals in their anhydrous and crystalline solvate forms (7). A significant body of literature has existed on the effect of solid state properties on solubility behavior and a wide range of materials that can retard phase transformations have been identified (8,9). The range of materials included polyvinylpyrrolidone, methylcellulose, acacia, gelatin, carboxymethylcellulose, pectin, sodium alginate, propylene glycol algin, and surfactants (8,9). However, little information is available on the identification of structure-based nucleation inhibitors. Sodium cholate was found to retard the particle growth and dissolution rate of cholesterol in a pH dependent fashion, while cholic acid catalyzes the nucleation process of cholesterol (10). Cortisone alcohol inhibited the phase transformation of cortisone acetate from the metastable to the water-stable form in aqueous suspensions (11). Recent work characterizing the crystallization of DMP 323 from a metastable Gelucire/polyethylene glycol semisolid matrix identified urea as a structure-based nucleation inhibitor that effectively stabilized the metastable system (12). As part of the development of a parenteral solution dosage form for intravenous administration, the solubility behavior of etanidazole was investigated. The objectives of this study were to evaluate the aqueous solubility of etanidazole, to characterize its crystalline phase transition and to evaluate structure-based mechanisms for formulation stabilization.

EXPERIMENTAL SECTION

Materials

Etanidazole (lot INY-Y191) was prepared by Chemie Linz AG, Linz, Austria and was used as received. Imidazole, ethanolamine and diethanolamine were used as received (Sigma). The water was house-deionized water that was passed through a Nanopure II (Barnstead) ion-exchange cartridge system and had a specific resistance of greater than 17 MΩ-cm. All solvents were HPLC grade. All other reagents were of analytical grade.

Polarized Light Microscopy

Microscopic observations were performed by suspending the sample in silicone immersion oil and examining with a polarized light microscope equipped with cross polars (Aristomet Microscope, Wild Leitz).

Thermal Analysis

The thermal properties were characterized with hot stage microscopy (Hot Stage FP82 and Central Processor FP80, Met-

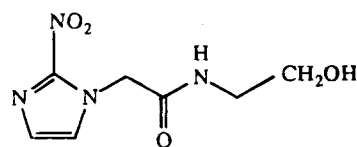


Fig. 1. Chemical structure of etanidazole.

¹ Pharmacy R&D, DuPont Merck Pharmaceutical Company, Wilmington, Delaware 19880-0400.

² To whom correspondence should be addressed.

ter) and differential scanning calorimetry (DSC 910 and Analyzer 2100, TA Instruments). Heating rates of 5°C/min or 10°C/min were employed for the techniques over a temperature range of 25–200°C.

X-ray Powder Diffraction

Powder x-ray diffraction data were obtained with an automated powder diffractometer (Model 3720, Phillips). The diffractometer was equipped with a variable slit, a scintillation counter and a graphite monochromator. The radiation was $\text{CuK}\alpha$ (40 kV, 30 mA). Data were collected at room temperature from 2–60 degrees 2θ ; step size was 0.02 degrees; count time was 0.5 sec. Powder samples were prepared as thin layers on glass or quartz specimen holders. The powder diffraction data have been deposited with the International Centre for Diffraction Data (Newtown Square, PA, 19073-3273, USA).

Coulometric Analysis

The water content was measured with direct coulometric analysis (Coulometer 684KF, Metrohm).

Aqueous Solubility

Solubility studies were carried out by placing excess etanidazole into a suitable container with the appropriate solvent and rotating end-to-end for twenty-four hours at the desired controlled temperature. The suspension was passed through a 0.2 μm filter (PVDF, Acrodisc LC13) with the first portion discarded to ensure saturation of the filter. The syringes and filters were equilibrated at the solubility study temperature prior to filtration. An aliquot of the filtrate was diluted and analyzed by HPLC and the remainder of the filtrate was employed for pH determination.

Nucleation Inhibition

Solutions of etanidazole at 50, 100, and 150 mg/mL were prepared in distilled water containing 1% imidazole or ethanolamine or 0.1% diethanolamine. The solutions were monitored for the formation of hydrate crystals at 4°C and 25°C.

Chromatographic Method

The concentration of etanidazole was determined with an isocratic HPLC method. Separation was achieved with a Waters $\mu\text{Bondapak}^{\text{®}}$ C₁₈, 30 cm \times 3.9 mm, with the temperature maintained at 35°C (Column Heater Module and Temperature Control Module, Waters Chromatography). The mobile phase was composed of acetonitrile: 0.01 M NaH_2PO_4 pH 4.6, (5:95). A flow rate of 1.0 mL/min was employed (HPLC Pump, Model 590, Waters Chromatography). Ultraviolet detection was utilized at 254 nm (Spectroflow 773 Absorbance Detector, Kratos Analytical Instruments). Chromatograms were recorded on an integrator (Model 3392A,

Hewlett Packard). The standards were freshly prepared before each analysis.

RESULTS AND DISCUSSION

Etanidazole was soluble in water with an equilibrium solubility of 68.1 mg/mL, pH 6.5. Changes in pH had a negligible effect on the solubility. The solubility was 65.2 mg/mL \pm 4.8 mg/mL (mean \pm SD, $n = 25$) over a pH range of 0.72 to 13.2. Etanidazole dissolved initially at concentrations in excess of 150mg/mL. However, as the etanidazole suspensions were rotated, the appearance of the solid phase changed from a fine powder to large fused crystals.

The solid phase was isolated and characterized by dissolving 15 grams of etanidazole in 100 milliliters of water. The etanidazole dissolved completely and no excess solid phase remained to contaminate the precipitate. The material appeared needle-shaped by polarized light microscopy with birefringence and distinct extinctions were observed when rotated under cross polars consistent with a crystalline material. Powder x-ray diffraction pattern confirmed that the isolated precipitate was crystalline. Comparison of the powder diffraction patterns of etanidazole and the isolated precipitate indicated changes in the crystalline form (Fig. 2). In the isolated precipitate (Fig. 2b), prominent additional signals appeared in the diffraction pattern at 10.1 degrees, 17.4 degrees, 18.2 degrees, 19.6 degrees, 35.2 degrees, 43.1 degrees and 56.6 degrees. In addition in the etanidazole drug substance (Fig. 2a), significant peaks disappeared at 16.6 degrees and 21.6 degrees when compared to the isolated precipitate. The HPLC retention time of the precipitate was in agreement with that of etanidazole. The precipitate contained 5.6% water as determined by coulometric analysis. DSC of the precipitate revealed two endothermic peaks at 64.1°C and 142.2°C (Fig. 3a) with hot stage microscopy observations consistent with evolution of water from 60–70°C and subsequent melting of the dehydrated precipitate at 140°C. Heating to 100°C in a vented pan, cooling to room temperature, and reheating to 200°C resulted in a thermogram with a single endothermic peak at 165.6°C (Fig. 3b) that was comparable to that of the “as received” drug substance. Thus, thermal dehydration and cooling permitted conversion of the precipitate to the “as received” drug substance as evidenced by the shift in the melting point, this behavior was confirmed with x-ray powder diffraction. The data indicated that the additional peak on differential scanning calorimetry analysis can be attributed to water of hydration, with the stoichiometry and powder x-ray diffraction suggesting a polymorphic monohydrate (**II**).

The solubility of **II** in water reached an equilibrium value of 68 mg/mL after 24 hours (Fig. 4). Therefore, the solubility studies were actually determining the solubility of the more stable **II**. The dissolution profiles of anhydrous etanidazole (**I**) and **II** were determined as a function of temperature and the maximum solubility values were employed for calculation of the thermodynamic parameters of the phase transition. The maximum solubility values were employed to generate the van't Hoff plot (Fig. 5). The transition temperature was 60.8°C and the ΔH_S was 7.4 kcal/mole and 12.7 kcal/mole for **I** and **II**, respectively. The enthalpy of hydration (ΔH_{HT}) was determined from the difference between the ΔH_S for **I** and **II** and was found

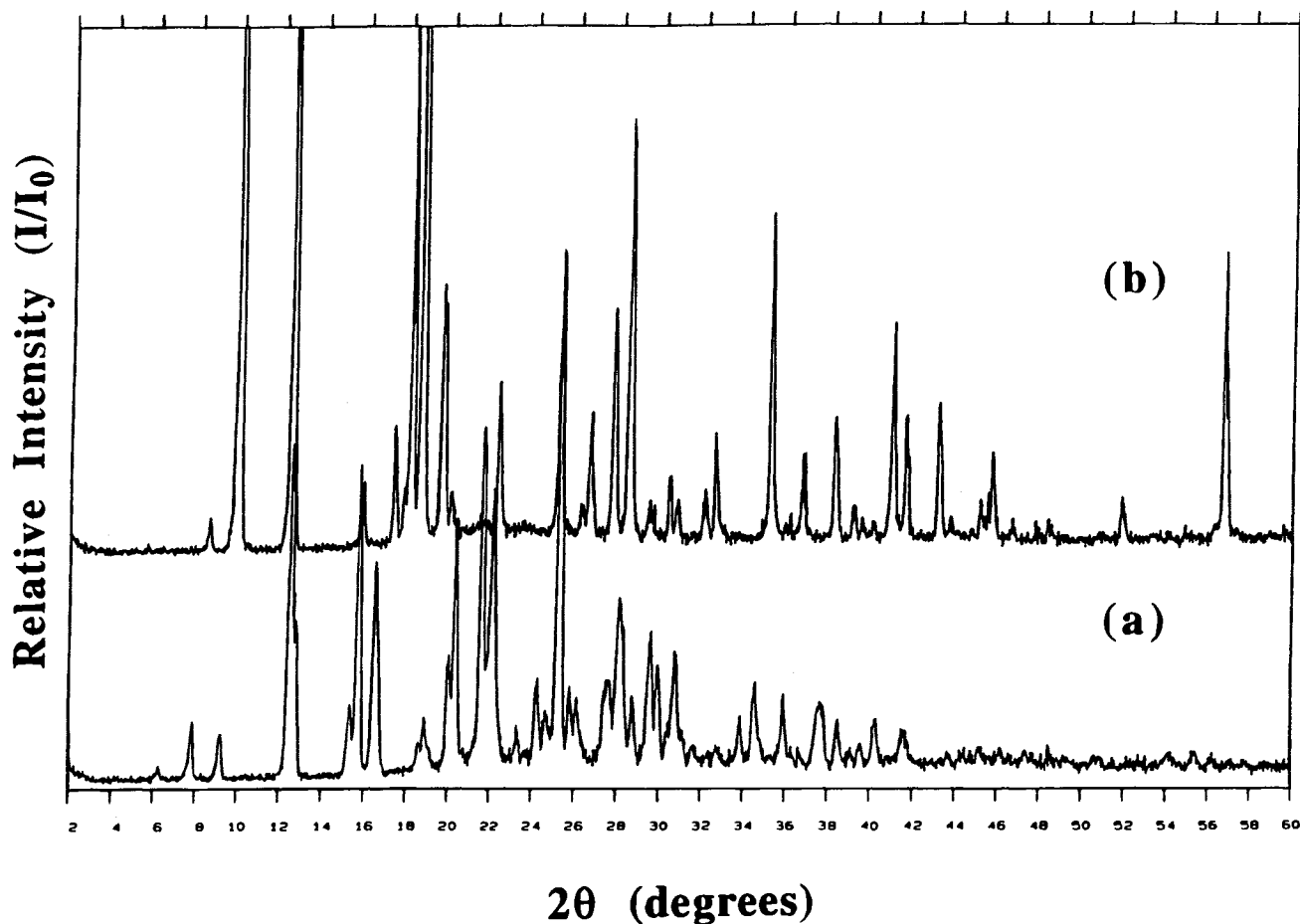


Fig. 2. Powder x-ray diffraction patterns for etanidazole as received (a) and the precipitate isolated from etanidazole studies (b).

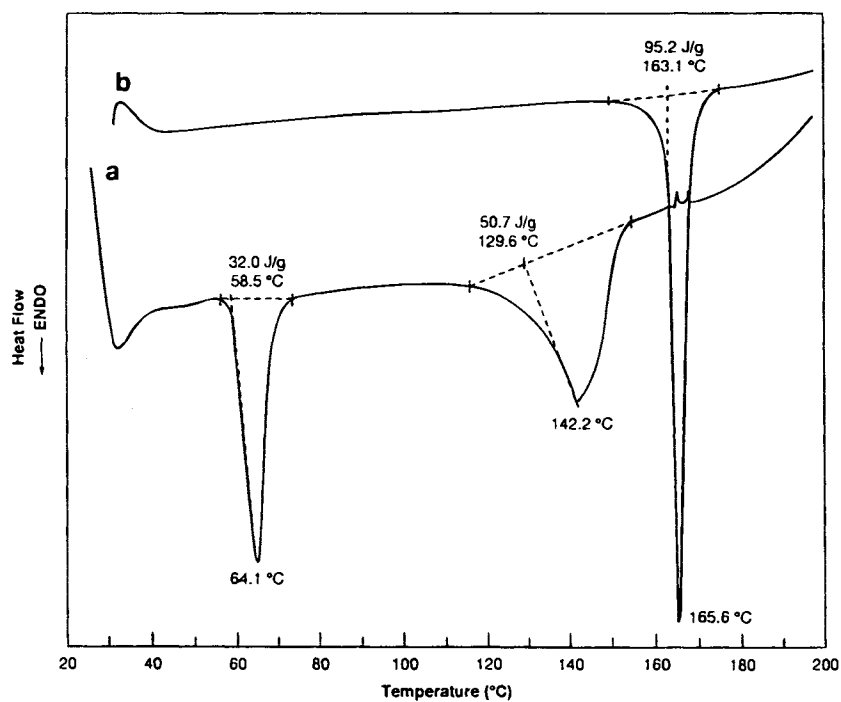
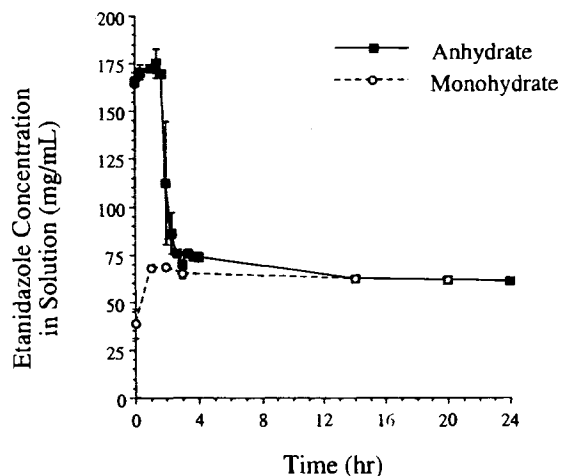


Fig. 3. DSC thermogram of the precipitate isolated from a saturated solution of etanidazole in a vented sample pan (a) and after heating to 100°C, cooling to room temperature and reheating (b) at 10°C/min.

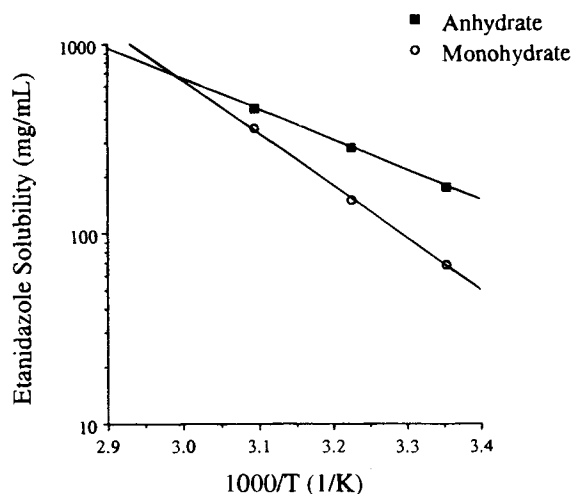
Table 1. Nucleation Inhibition of Etanidazole Hydrate from Aqueous Etanidazole Solutions After Six Months at 4°C and 25°C

Etanidazole (M)	Control		Imidazole 0.15 M		Nucleation Inhibitor Ethanolamine 0.16 M		Diethanolamine 0.0095 M	
	4°C	25°C	4°C	25°C	4°C	25°C	4°C	25°C
0.23	PPT	Clear	Clear	Clear	Clear	Clear	Clear	Clear
0.47	PPT	PPT	Clear	Clear	PPT	Clear	PPT	Clear
0.70	PPT	PPT	PPT	Clear	PPT	PPT	PPT	PPT

**Fig. 4.** The dissolution profiles of the anhydrate and monohydrate of etanidazole in distilled water as a function of time at 25°C. The data points and error bars represent the mean and standard deviation of three replicates.

to be -5.3 kcal/mole. The free energy and entropy of the hydration process at 25°C were calculated by standard methods and found to be 560 cal/mole and -19.6 cal/mole. $^{\circ}$ K (7).

Etanidazole solutions prepared at 50 mg/mL and autoclaved, did not precipitate on storage at 4°C, while precipitation was observed in 38% of non-autoclaved samples. In addition,

**Fig. 5.** The van't Hoff plot for the anhydrate and monohydrate of etanidazole in water. The data points represent the mean of three replicates.

trace degradation via amide hydrolysis to 2-nitro-1*H*-imidazole-1-acetate and ethanolamine occurred following autoclaving (13). The trace degradants may be effectively acting as inhibitors of the hydrate nucleation.

Etanidazole solutions at 0.23 M, 0.47 M and 0.70 M (50, 100 and 150 mg/mL, respectively) were prepared without nucleation inhibitor or with the addition of 0.15 M (1.0%) imidazole, 0.16 M (1.0%) ethanolamine or 0.0095 M (0.1%) diethanolamine and the physical stability was monitored at 4°C and 25°C (Table I). In the absence of nucleation inhibitors, **II** precipitated within eight hours from 0.23 M, 0.47 M and 0.70 M etanidazole solutions at 4°C and from 0.47 M and 0.70 M etanidazole solutions at 25°C. Etanidazole solutions at 0.23 M, 0.47 M and 0.70 M were physically stable in the presence of 0.15 M imidazole at 25°C. At 4°C, the 0.70 M solution formed **II** while the 0.23 M and 0.47 M solutions remained stable for over six months with 0.15 M imidazole. In the presence of 0.16 M ethanolamine or 0.0095 M diethanolamine, etanidazole was physically stable at 0.23 M and 0.47 M at 25°C while the 0.70 M solution **II** precipitated. At 4°C, the 0.47 M and 0.70 M solutions formed **II** while the 0.23 M solution remained stable for over six months.

I underwent a transition in aqueous solutions to the more thermodynamically stable **II** when the solubility of **II** was exceeded. The physical stability of etanidazole solutions at 4°C was improved following autoclaving. The addition of structural analogs of the trace degradation products that formed following autoclaving provided effective nucleation inhibition of **II**. Even at concentrations where **II** would be expected to form, the nucleation inhibitors effectively stabilized the metastable systems. Thus, the ability to inhibit crystal formation from metastable solutions has been demonstrated successfully with a series of specific structure-based nucleation inhibitors.

REFERENCES

1. C. N. Coleman, R. C. Urtasun, T. H. Wasserman, S. Hancock, J. W. Harris, J. Halsey and V. K. Hirst. Initial Report of the Phase I Trial of the Hypoxic Cell Radiosensitizer SR-2508. *Int. J. Radiat. Oncol. Biol. Phys.* **10**:1749-1753 (1984).
2. P. J. O'Dwyer, F. P. LaCreta, J. Walczak, T. Cox, S. Litwin, J. P. Hoffman, M. Jimmy and R. L. Comis. Phase I/Pharmacokinetic/Biochemical Study of the Nitroimidazole Hypoxic Cell Sensitizer SR2508 (Etanidazole) in Combination with Cyclophosphamide. *Brit. J. Cancer* **68**:756-766 (1993).
3. G. E. Adams and I. J. Stratford. Hypoxic-Mediated Nitroheterocyclic Drugs in the Radio- and Chemotherapy of Cancer: An Overview. *Biochem. Pharmacol.* **35**:71-76 (1986).
4. J. J. Clement, M. S. Gorman, I. Wodinsky, R. Catane and R. K. Johnson. Enhancement of Antitumor Activity of Alkylating Agents by the Radiation Sensitizer Misonidazole. *Cancer Res.* **40**:4165-4172 (1980).

5. M. E. Varnes, J. E. Biaglow, C. J. Koch and E. J. Hall. Depletion of Non-Protein Thiols of Hypoxic Cells by Misonidazole and Metronidazole. In L. L. Brady (ed.), *Radiation Sensitizers: Their Use in the Clinical Management of Cancer*, Masson Publishing, New York, 1990, pp. 121–126.
6. K. S. Kumar and J. F. Weiss. Inhibition of Glutathione Peroxidase and Glutathione Transferase in Mouse Liver by Misonidazole. *Biochem. Pharmacol.* **35**:3143–3146 (1986).
7. E. Shefter and T. Higuchi. Dissolution Behavior of Crystalline Solvated and Nonsolvated Forms of Some Pharmaceuticals. *J. Pharm. Sci.* **52**:781–791 (1963).
8. W. L. Chiou and S. Riegelman. Pharmaceutical Applications of Solid Dispersion Systems. *J. Pharm. Sci.* **60**:1281–1302 (1971).
9. E. Shefter. Solubilization by Solid-State Manipulation. In S. H. Yalkowsky (ed.), *Techniques of Solubilization of Drugs*, Volume 12 in *Drugs and the Pharmaceutical Sciences*, Marcel Dekker, New York, 1981, pp. 159–182.
10. H. Y. Saad and W. I. Higuchi. Cholesterol Particle Growth and Dissolution Rates. II. Retardation Effects of Cholate. *J. Pharm. Sci.* **54**:1303–1307 (1965).
11. J. E. Carless, M. A. Moustafa and H. D. C. Rapson. Effect of Crystal Form, Cortisone Alcohol and Agitation on Crystal Growth of Cortisone Acetate in Aqueous Suspensions. *J. Pharm. Pharmac.* **20**:639–645 (1968).
12. M. B. Maurin and R. D. Vickery. Solubility Behavior and Structure-Based Nucleation Inhibition of a Cyclic Urea HIV-1 Protease Inhibitor in a Semi-solid Matrix. Submitted for publication.
13. S. M. Rowe, M. B. Maurin and M. A. Hussain. Solution Stability of Etanidazole (DuP 435). *Pharm. Res.* **10**:S-228 (1993).